A Theoretical Study on Spin-Dependent Transport of "Ferromagnet/Carbon Nanotube Encapsulating Magnetic Atoms/Ferromagnet" Junctions with 4-Valued Conductances

Satoshi KOKADO[1,2] * and Kikuo HARIGAYA[2,3] †

[1]*Faculty of Engineering, Shizuoka University, Hamamatsu 432-8561, Japan*
[2]*Nanotechnology Research Institute, AIST, Tsukuba 305-8568, Japan*
[3]*Synthetic Nano-Function Materials Project, AIST, Tsukuba 305-8568, Japan*

(February 2, 2008)

Abstract

As a novel function of ferromagnet (FM)/spacer/FM junctions, we theoretically investigate multiple-valued (or multi-level) cell property, which is in principle realized by sensing conductances of four states recorded with magnetization configurations of two FMs; (up,up), (up,down), (down,up), (down,down). In order to sense all the states, 4-valued conductances corresponding to the respective states are necessary. We previously proposed that 4-valued conductances are obtained in FM1/spin-polarized spacer (SPS)/FM2 junctions, where FM1 and FM2 have different spin polarizations, and the spacer depends on spin [J. Phys.: Condens. Matter **15**, 8797 (2003)]. In this paper, an ideal SPS is considered as a single-wall armchair carbon nanotube encapsulating magnetic atoms, where the nanotube shows on-resonance or off-resonance at the Fermi level according to its length. The magnitude of the obtained 4-valued conductances has an opposite order between the on-resonant nanotube and the off-resonant one, and this property can be understood by considering electronic states of the nanotube. Also, the magnetoresistance ratio between (up,up) and (down,down) can be larger than the conventional one between parallel and anti-parallel configurations.

*Electronic mail: tskokad@ipc.shizuoka.ac.jp

†Electronic mail: k.harigaya@aist.go.jp

I. INTRODUCTION

Spin polarized junctions (SPJ) such as ferromagnet(FM)/spacer/FM junctions [1–4] have been recently applied to elements in magnetic random access memories (MRAM) because of their magnetoresistance (MR) effect, which appears when an applied magnetic field changes an angle between magnetizations of two FMs. In the practical use, a spin-valve type, which corresponds to a memory cell of 2 values (1bit) represented by "0" and "1" [5], is usually adopted. For the writing process, the magnetization of only one side of the FM is changed under the applied field so that magnetization configurations between two FMs are parallel (P) or anti-parallel (AP). For the reading process, we use the difference in resistance between the P and AP configurations, the so-called MR effect.

For the SPJ, much effort has been made to develop elements in high density memories, which also have high sensitivity for the reading process. Important factors are considered to be (a) large MR ratio, whose expression in the unit of percent is defined by $100 \times (\Gamma_P - \Gamma_{AP})/\Gamma_{AP}$ with $\Gamma_{P(AP)}$ being conductance of the P (AP) case, and (b) ultra small junctions. The realistic SPJ for (a) can be, for example, Co-Fe/Al-O/Co-Fe junctions with the MR ratio of 60% at room temperature [2], epitaxially grown $Ga_{1-x}Mn_xAs/AlAs/Ga_{1-x}Mn_xAs$ junctions with the MR ratio more than 70% at 8 K [3], and Co/Fe-doped $Al_2O_3/Ni_{80}Fe_{20}$ junctions, whose MR ratio was enhanced as compared to the case of an undoped Al_2O_3 [4]. On the other hand, candidates of the SPJ for (b) may be FM/nanowire/FM junctions and FM/carbon nanotube/FM junctions [6–11], where it should be noted that the nanotube length is about 200 nm [7,8] or 250nm [6] in actual experiments and their size is very large at the present moment. In the further, however, we appear to see many problems with how to miniaturize the junctions, because challenges for the limits of the junctions size will be more and more severe in spite of the progress of experimental techniques.

Studies from another viewpoints far from the miniaturization should be necessary simultaneously. In fact, for other memories [12] such as the Flash memory [13], multiple valued (or multi-level) cell property [13], which allows the plural bits to be stored in each memory cell and accordingly reduces the memory cell size by 1/(the number of bits), has been extensively studied. On the other hand, there are few studies for the SPJ. If such a property is included in the SPJ, they will function as an memory cell, which is more efficient than the conventional one.

We here describe the multiple-valued cell property in the general SPJ, based on our previous study [14]. In a possible scheme, recorded states are supposed to be four magnetization configurations of two FMs consisting of (up,up), (up,down), (down,up), (down,down), which are obtained by applying the magnetic fields to the respective FMs. The junctions correspond just to 2bits memory cells. Then, in order to sense all the states, 4-valued conductances corresponding to the respective states are obviously necessary. By paying attention to the magnitude of total magnetization in the whole system, a model to obtain such conductances is considered to be FM1/spin-polarized spacer (SPS)/FM2 junctions, where the FM1 and FM2 have different spin polarizations [15], according to the following procedure. First, a difference of conductances between (up,up) and (down,down) will appear, if the spacer is the SPS, where magnetization in the spacer is pinned. Second, a difference between (up,down) and (down,up) will be obtained by introducing the FM1 and FM2, in addition to the above mentioned SPS.

In this paper, as an ideal SPS to observe 4-valued conductances, we adopt a single-wall armchair carbon nanotube encapsulating magnetic atoms [16,17], and investigate the spin dependent transport of "FM1/single-wall armchair carbon nanotube encapsulating magnetic atoms/FM2" junctions using the Green's function technique. When all spins of magnetic atoms are pinned parallel to the magnetization axes of FM1 and FM2, 4-valued conductances are explicitly obtained at a certain value of an exchange interaction between conduction electron spin and spin of magnetic atoms. The magnitude of the obtained 4-valued conductances has an opposite order between the nanotube with on-resonant behavior and that with off-resonant behavior. Also, the MR ratio between $\Uparrow,\Uparrow$ and $\Downarrow,\Downarrow$ can be larger than the conventional one between P and AP configurations.

II. IDEAL SPIN POLARIZED SPACERS TO OBTAIN 4-VALUED CONDUCTANCES

We first consider ideal SPSs to certainly observe 4-valued conductances. In the previous study [14], we found that 4-valued conductances tend to be obtained in the case of largely spin-polarized spacer with

$$\frac{T_{\uparrow,\uparrow} - T_{\downarrow,\downarrow}}{T_{\uparrow,\uparrow}} \sim 1, \tag{1}$$

where $T_{\uparrow,\uparrow}$ and $T_{\downarrow,\downarrow}$ are transmission coefficients of spin-up and spin-down, respectively, in an expression of the conductance [18,19],

$$\Gamma = \frac{4\pi^2 e^2}{h} \sum_{\sigma=\uparrow,\downarrow} \sum_{\sigma'=\uparrow,\downarrow} T_{\sigma,\sigma'} D_{1,\sigma}(E_{\mathrm{F}}) D_{2,\sigma'}(E_{\mathrm{F}}), \tag{2}$$

with σ ($=\uparrow$ or $\downarrow$) being spin of the conduction electron, $D_{1(2),\sigma}(E)$ being the local density-of-states (DOS) at an interfacial layer in FM1(2) at the Fermi level E_{F}, and $T_{\sigma,\sigma'}$ being a spin dependent transmission coefficient including spin-flip process of $\sigma \neq \sigma'$. Based on the fact, we give four objectives for the spacer having magnetic atoms, which are

(i) to strongly pin the magnetization of magnetic atoms in the spacer parallel to magnetization axes of FMs,

(ii) to diminish magnetic couplings between magnetic atoms and FMs,

(iii) to make effective couplings between the conduction electron spin and spins of magnetic atoms, which act as much as possible,

(iv) to have a long spin-flip scattering length to conserve the spin of conduction electron through the spacer.

As for (i), we propose that a coercive field of magnetic particles consisting of magnetic atoms is much higher than ones of FMs. For (ii), we suppose that distances between magnetic atoms and FMs should be controlled so that magnetic dipole-dipole interactions between them become very small and give little influence on the spin dependent conduction. In (iii),

3

we should make a situation so that electrons in all conduction routes can interact with spins of magnetic atoms. For (iv), it is desired that the spin-orbit interaction of a material of the spacer is very small.

As a realistic SPS, which could satisfy such objectives, we bear in mind of a carbon nanotube encapsulating magnetic atoms [16,17] by the following reasons: First, the size of a particle consisting of magnetic atoms may be close to that of a single domain particle by tuning conditions of fabrication, where the single domain particle has a high coercive field. The coercive field was recently observed as about 0.5 kOe at 300 K even for Fe particles encapsulated with non-single domain size of about 70 nm [16]. Furthermore, for only the magnetic particle, it was experimentally shown that the Fe_2O_3 nanoparticle with the diameter of 6.3 nm has the coercive field of 1 kOe at 300 K [20]. If such the particle can be encapsulated in the nanotube, the nanotube will act as the ideal SPS. Second, magnetic atoms can be encapsulated in the inner region of the nanotube [16], where distances between the atoms and nanotube edges could be tuned by controlling nanotube growth processes. Third, since the encapsulated magnetic atoms are completely surrounded by carbon atoms, electrons in all conduction routes can interact with spins of magnetic atoms. Here, magnitude of couplings may be also tunable by controlling nanotube growth processes, because they strongly depend on distances between carbon atoms and magnetic atoms. Fourth, the nanotube itself has very long spin-flip scattering lengths which extend to 130 nm at least [6].

III. "FM1/CARBON NANOTUBE ENCAPSULATING MAGNETIC ATOMS/FM2" JUNCTIONS

A. Model and method

We focus on "FM1/single-walled armchair carbon nanotube encapsulating magnetic atoms/FM2" junctions, where magnetic atoms are located in the center of the nanotube. Figure 1 shows a simplified model, in which the FM has a simple cubic structure, the x-direction of FMs is set to be semi-infinite, and their yz-directions have the periodic boundary condition by being regarded as an infinite system. The armchair nanotube has a finite length, and then it is regarded just as an armchair ribbon [21] with short periodicity. The each edge carbon atom of the nanotube is assumed to interact with its nearest atom of the cubic lattice of the FM. On the other hand, the encapsulated magnetic atoms have localized spins. We here assume that their spins are divided into several spin clusters which interact with their nearest carbon atoms respectively, and all the spin clusters have the identical total spin. The total spin is approximately represented by a classical spin $\mathbf{S}$ on the assumption that the spin cluster consists of many spins, and further every $\mathbf{S}$ is set to have the same direction. Now, each $\mathbf{S}$ is arrayed along two dimer lines of the nanotube, and it has one to one interaction with carbon atoms in their lines. According to the theory on magnetic impurity problem [22], we take into account antiferromagnetic exchange interactions between conduction electron spins and $\mathbf{S}$'s, where all the exchange interactions are here set to be same. Also, interactions between $\mathbf{S}$'s and spins of FMs are neglected by assuming that they have little influence on the spin dependent conduction, under a balance between their coercive fields and magnetic fields due to respective spins. The balance is actually sensitive to distances between magnetic atoms and FMs.

Using a single orbital tight-binding model with nearest neighbor transfer integrals, the Hamiltonian is given by,

$$H_{total} = H + V, \tag{3}$$

$$H = H_1^0 + H_2^0 + H_{NT}, \tag{4}$$

$$H_{NT} = H_{NT}^0 + H_{mag}, \tag{5}$$

with

$$H_u^0 = \sum_{i \in u} \sum_{\sigma} e_{i,\sigma} c_{i,\sigma}^\dagger c_{i,\sigma} + \sum_{\langle i,j \rangle \in u} \sum_{\sigma} \left(t_{i,j} c_{i,\sigma}^\dagger c_{j,\sigma} + \text{h.c.} \right), \tag{6}$$

for u=1, 2, NT,

$$H_{mag} = \sum_{i \in mag} \left(\Delta e \sum_{\sigma} c_{i,\sigma}^\dagger c_{i,\sigma} - J \sum_{\sigma,\sigma'} \sigma_{\sigma,\sigma'} \cdot \mathbf{S} c_{i,\sigma}^\dagger c_{i,\sigma'} \right), \tag{7}$$

$$V = \sum_{\langle i,j \rangle} \sum_{\sigma} \left(v_{i,j} c_{i,\sigma}^\dagger c_{j,\sigma} + \text{h.c.} \right), \tag{8}$$

where $H_{1(2)}^0$ is Hamiltonian for the FM1 (FM2), H_{NT}^0 is that for the carbon nanotube, and H_{mag} denotes interactions between the encapsulated magnetic atoms and the respective nearest carbon atoms, where $\sum_{i \in mag}$ means that the summation is taken for carbon atoms interacting with magnetic atoms. The term V represents couplings between FMs and the nanotube, where the each edge carbon atom of the nanotube couples to its nearest atom of the cubic lattice of the FM. Here, $c_{i,\sigma}$ ($c_{i,\sigma}^\dagger$) is the annihilation (creation) operator of an electron with spin-σ (=↑ or ↓) at the i-th site, $t_{i,j}$ and $v_{i,j}$ are transfer integrals between the i-th site and the j-th site, and $e_{i,\sigma}$ denotes the on-site energy for spin-σ at the i-th site. Furthermore, Δe is the difference of energy between the pure carbon atom and the carbon atom interacting with the magnetic atoms, J is the antiferromagnetic exchange integral with negative sign [22], and $\sigma_{\sigma,\sigma'}$ is the (σ, σ') component of the Pauli matrix for the conduction electron spin. Also, $\mathbf{S}$ $[= (S_x, S_y, S_z)]$ represents the classical spin with $S \equiv |\mathbf{S}|$.

Within the Green's function technique [18,19], we calculate the conductance at zero temperature, which is written by,

$$\Gamma = \frac{4\pi^2 e^2}{h} \text{Tr}[\hat{D}_1 \hat{T}^\dagger \hat{D}_2 \hat{T}], \tag{9}$$

$$\hat{T} = V + VG^\dagger V, \tag{10}$$

$$G = (E_F + \text{i}0 - H_{total})^{-1}, \tag{11}$$

with

$$\hat{D}_u = -\frac{1}{\pi} \text{Im} G_u^0, \tag{12}$$

$$G_u^0 = (E_F + \text{i}0 - H_u^0)^{-1}, \tag{13}$$

5

for u=1, 2. Here, $\hat{D}_{1(2)}$ is the density-of-states (DOS) operator at E_{F} of the FM1(2), and $\hat{T}$ is the T-matrix. We below name Γ for the respective magnetization configurations as $\Gamma_{m1,m2}$, where $m1$ ($m2$) is the magnetization state of FM1 (FM2), which is $\Uparrow$ or $\Downarrow$.

Using these conductances, we obtain the MR ratio in the unit of percent, which is defined by

$$R_{m1,m2} = 100 \times \frac{\Gamma_{\Downarrow,\Downarrow} - \Gamma_{m1,m2}}{\Gamma_{\Downarrow,\Downarrow}}, \tag{14}$$

where $m1$ ($m2$) is the magnetization state of FM1 (FM2) with $\Uparrow$ or $\Downarrow$.

In this calculation, we choose parameters as follows: We set $t_{i,j} = t \ (< 0)$ [23] and $v_{i,j} = 0.1t$, assuming that v is smaller than t because of different types between two orbitals, imperfect lattice matches at the interface, and so on. When E_{F}=0, $e_{i,\uparrow}/|t|$ ($e_{i,\downarrow}/|t|$) is 5.1 (5.7) for the FM1 and 5.175 (5.625) for the FM2 [24], by considering that the s-orbital, which is spin-polarized by coupling to the localized d-orbitals, contributes to the transport of the FMs. The spin polarization [15] at the interfacial layer of the FM1 (FM2) at E_{F}, P_1 (P_2), is then evaluated to be about 0.45 (0.25) [25]. For the carbon atom, $e_{i,\uparrow}/|t|$ ($e_{i,\downarrow}/|t|$) is set to be 0 (0) by focusing on its π orbital. By taking into account that the π orbital is coupled to d-orbitals of the magnetic atoms, whose energies are lower than $e_{i,\uparrow}/|t|$ and $e_{i,\downarrow}/|t|$ of the π orbital, $\Delta e/|t|$ is considered to be positive and it is put as 0.2. Also, the number of unit cells in the circumference direction of the nanotube is 10. The number of dimer lines [21] N is 20, 21, and 22, which correspond to nanotubes with the on-resonance, the off-resonance, and the off-resonance at E_{F}, respectively [10,21]. It is well known that the armchair nanotube shows the on-resonant behavior for $N = 3M - 1$, the off-resonant one for $N = 3M$, and the off-resonant one for $N = 3M + 1$, respectively, with M being an integer [10,21]. For N=20 and 21, the spin, $\mathbf{S}$, is arrayed at each carbon atom in 10-th and 11-th dimer lines of the nanotube, while it is arrayed at each carbon atom in its 11-th and 12-th dimer lines for N=22. In each N, the number of $\mathbf{S}$'s is 40, which is obtained from the relation of (the number of unit cells in the circumference direction of the nanotube) $\times$ (the number of dimer lines with $\mathbf{S}$'s) $\times$ (the number of sublattices in the unit cell)= $10 \times 2 \times 2$. Furthermore, $\mathbf{S}$'s are considered to exist parallel to yz-plane, and an angle between $\mathbf{S}$'s and z-axis is written as θ.

B. Calculated results and considerations

In the upper panel of Fig. 2(a), we show $-JS/|t|$ dependence of the conductance, $\Gamma_{m1,m2}$, for θ=0 in the case of N=20. At $JS/|t|$=0, $\Gamma_{m1,m2}$ has a difference only between P and AP configurations. For $JS/|t| \neq 0$, differences among all conductances appear, and become largest in the vicinity of $JS/|t|$=−0.2. Also, $\Gamma_{m1,m2}$ has a relation of $\Gamma_{\Downarrow,\Downarrow} > \Gamma_{\Uparrow,\Downarrow} > \Gamma_{\Downarrow,\Uparrow} > \Gamma_{\Uparrow,\Uparrow}$ for a wide range of $-0.8 < JS/|t| < 0$.

The middle and lower panels of Fig. 2(a) show $\Gamma_{m1,m2}$ for θ=0 in the case of N=21 and 22, respectively. In the case of N=21, differences among all conductances become large in the vicinity of $JS/|t|$=−0.4, while they do in the vicinity of $JS/|t|$=−0.75 in the case of N=22. It should be noted that $\Gamma_{m1,m2}$ of N=21 and 22 has a relation of $\Gamma_{\Uparrow,\Uparrow} > \Gamma_{\Downarrow,\Uparrow} > \Gamma_{\Uparrow,\Downarrow} > \Gamma_{\Downarrow,\Downarrow}$ for a wide range of $-0.8 < JS/|t| < 0$, and its order is opposite to that of N=20.

The behavior of conductances can be understood by considering electronic states in the center of the nanotube, where magnetic atoms are encapsulated. We therefore investigate the local DOS, defined by,

$$\text{Local DOS} = -\frac{1}{\pi}\text{Im}\sum_{i\in mag}\langle i|(E_{\text{F}} + \text{i}0 - H_{NT})^{-1}|i\rangle, \tag{15}$$

where $|i\rangle$ represents the orbitals of carbon atoms interacting with magnetic atoms, and $\sum_{i\in mag}$ means that the summation is taken for those carbon atoms.

In the upper, middle, lower panels of Fig. 3(a), we show the local DOS for $\Delta e/|t|=0$ and $JS/|t|=0$, $\Delta e/|t|=0.2$ and $JS/|t|=0$, and $\Delta e/|t|=0.2$ and $JS/|t|=-0.2$, respectively, in the case of $N=20$. For $\Delta e/|t|=0$ and $JS/|t|=0$, i.e., the case of no encapsulated atoms, small peaks of spin-up and spin-down are found at E_{F} ($=0$), as shown in the upper panel of Fig. 3(a). The feature just represents the on-resonance at E_{F}. The peaks originate from wave functions at the Gamma point [21], which are delocalized over the whole nanotube. For $\Delta e/|t|=0.2$ and $JS/|t|=0$, i.e., the case of encapsulated nonmagnetic atoms, the peaks of spin-up and spin-down are shifted to higher energy with the same magnitude [see middle panel of Fig. 3(a)]. Then, 2-valued conductances are obtained because of no difference of local DOSs between spin-up and spin-down. On the other hand, for $\Delta e/|t|=0.2$ and $JS/|t|=-0.2$, i.e., the case of encapsulated magnetic atoms, the peak of spin-down is close to E_{F} as shown in the lower panel of Fig. 3(a). Since the electron favors to transmit when the DOS is large around E_{F}, transmission of spin-down electron increases compared to that of spin-up electron. By taking into account the spin dependent DOSs of FMs with $P_1=0.45$ and $P_2=0.25$, $\Gamma_{\Downarrow,\Downarrow}$ ($\Gamma_{\Uparrow,\Uparrow}$) becomes largest (smallest) in all conductances, while $\Gamma_{\Uparrow,\Downarrow}$ and $\Gamma_{\Downarrow,\Uparrow}$ are present between $\Gamma_{\Downarrow,\Downarrow}$ and $\Gamma_{\Uparrow,\Uparrow}$, and $\Gamma_{\Uparrow,\Downarrow} > \Gamma_{\Downarrow,\Uparrow}$ is realized also.

The upper, middle, lower panels of Fig. 3(b) show the local DOS for $\Delta e/|t|=0$ and $JS/|t|=0$, $\Delta e/|t|=0.2$ and $JS/|t|=0$, $\Delta e/|t|=0.2$ and $JS/|t|=-0.4$, respectively, in the case of $N=21$. In the upper panel of Fig. 3(b), no peaks are found at E_{F} for $\Delta e/|t|=0$ and $JS/|t|=0$. It represents the off-resonance at E_{F}. By setting $\Delta e/|t|=0.2$ and $JS/|t|=0$, peaks of spin-up and spin-down near E_{F} are shifted to higher energy with the same magnitude as shown in middle panel of Fig. 3(b), and then 2-valued conductances are obtained. For $\Delta e/|t|=0.2$ and $JS/|t|=-0.4$, the peak of spin-up appears in the vicinity of E_{F} [see the lower panel of Fig. 3(b)]. Therefore, based on the DOSs of the FMs, $\Gamma_{\Uparrow,\Uparrow}$ ($\Gamma_{\Downarrow,\Downarrow}$) is largest (smallest) in all conductances, while $\Gamma_{\Uparrow,\Downarrow}$ and $\Gamma_{\Downarrow,\Uparrow}$ are present between $\Gamma_{\Uparrow,\Uparrow}$ and $\Gamma_{\Downarrow,\Downarrow}$, and also $\Gamma_{\Downarrow,\Uparrow} > \Gamma_{\Uparrow,\Downarrow}$ is realized. The case of $N=22$ can be understood based on the local DOSs shown in Fig. 3(c), too.

We systematically understand the above peak shifts as follows: When the carbon atom interacts with the magnetic atoms, its energy levels of spin-up are shifted to high energy, while its energy levels of spin-down are not largely altered, owing to $\Delta e/|t| > 0$ and $JS/|t| < 0$. For the on-resonant nanotube, in which energy levels of spin-up and spin-down exist at E_{F} for $\Delta e/|t|=JS/|t|=0$, the energy levels of spin-down are closer to E_{F} than those of spin-up when $\Delta e/|t| > 0$ and $JS/|t| < 0$. On the other hand, for the off-resonant nanotube, in which no energy levels of spin-up and spin-down exist at E_{F} for $\Delta e/|t|=JS/|t|=0$, the energy levels of spin-up near the top of the valence band approach to E_{F} by setting $\Delta e/|t| > 0$ and $JS/|t| < 0$.

The MR ratio $R_{m1,m2}$ is shown in Fig. 2(b). In all panels, at $JS/|t|=0$, $R_{m1,m2}$ is finite

only between P and AP configurations and $|R_{m1,m2}|$ is about 15%. For a wide range of $-0.8 < JS/|t| < 0$, $|R_{m1,m2}|$ between P and AP configurations can be more than 15%. It should be emphasized that $|R_{m1,m2}|$ between $\Uparrow,\Uparrow$ and $\Downarrow,\Downarrow$ is larger than the conventional one between P and AP configurations. This feature is consistent with results for the case of the largely spin-polarized spacer with $(T_{\uparrow,\uparrow} - T_{\downarrow,\downarrow})/T_{\uparrow,\uparrow} \sim 1$ in the previous work [14]. Also, it is characteristic that for a wide range of $-0.8 < JS/|t| < 0$, $R_{m1,m2}$'s of N=20 and N=21 and 22 exhibit the positive MR and the negative one, respectively, reflecting the opposite order of $\Gamma_{m1,m2}$ between them.

In the following, we consider the θ dependence of $\Gamma_{m1,m2}$ and $R_{m1,m2}$, shown in Figs. 4(a) and (b), respectively. In each figure, the upper, middle, and lower panels are cases of $JS/|t|=-0.2$ of N=20, $JS/|t|=-0.4$ of N=21, and $JS/|t|=-0.8$ of N=22, respectively. A condition of $\theta/\pi=-0.5$ (0) represents that **S**'s are oriented in the $-y$ (z) direction. In all panels, at $\theta/\pi = -0.5$, only the difference of $\Gamma_{m1,m2}$ between the P and AP configurations is present, and then $|R_{m1,m2}|$ between them takes small values of less than 5 %, because of the spin-flip transmission. As θ approaches to 0, differences of $\Gamma_{m1,m2}$ among all configurations become large, because a difference of diagonal elements of $\hat{T}$ with regards to spin between spin-up and spin-down increases. Further, $|R_{m1,m2}|$ between $\Uparrow,\Uparrow$ and $\Downarrow,\Downarrow$ increases, too.

IV. CONCLUSION

For "FM1/armchair carbon nanotube encapsulating magnetic atoms/FM2" junctions, we theoretically investigated the multiple-valued cell property, which is in principle realized by sensing four states recorded with the magnetization configurations of two FMs. The obtained 4-valued conductances are strongly influenced by electronic states of the nanotube, and directions of spins of magnetic atoms. The order of magnitude of 4-valued conductances is opposite between the on-resonant nanotube and the off-resonant one. Furthermore, the MR ratio between (up,up) and (down,down) can be larger than the conventional one between P and AP configurations.

From the viewpoint of device applications, we expect that the present junctions will be a candidate for elements of the 2bits/cell MRAM. At the same time, the junctions with magnetization reversals between $\Uparrow,\Uparrow$ and $\Downarrow,\Downarrow$ may be more efficient magnetic sensor than the conventional spin-valve type [5], in the case of the largely spin-polarized spacer.

V. ACKNOWLEDGEMENTS

REFERENCES

[1] T. Miyazaki and N. Tezuka, J. Magn. Magn. Mater. **139**, L231 (1995); J. S. Moodera, L. R. Kinder, T. M. Wong, and R. Meservey, Phys. Rev. Lett. **74**, 3273 (1995).

[2] M. Tsunoda, K. Nishikawa, S. Ogata, and M. Takahashi, Appl. Phys. Lett. **80**, 3135 (2002).

[3] M. Tanaka and Y. Higo, Phys. Rev. Lett. **87**, 026602 (2001).

[4] R. Jansen and J. S. Moodera, Appl. Phys. Lett. **75**, 400 (1999).

[5] For example, see S. S. Parkin, K. P. Roche, M. G. Samant, P. M. Rice, R. B. Beyers, R. E. Scheuerlein, E. J. O'Sullivan, S. L. Brown, J. Bucchigano, D. W. Abraham, Yu. Lu, M. Rooks, P. L. Trouilloud, R. A. Wanner, W. J. Gallagher, J. Appl. Phys. **85**, 5828 (1999).

[6] K. Tsukagoshi, B. W. Alphenaar, and H. Ago, Nature **401**, 572 (1999).

[7] B. Zhao, I. Mönch, T. Mühl, H. Vinzelberg, and C. M. Schneider, Appl. Phys. Lett. **80**, 3144 (2002).

[8] B. Zhao, I. Mönch, T. Mühl, H. Vinzelberg, and C. M. Schneider, J. Appl. Phys. **91**, 7026 (2002).

[9] J. -R. Kim, H. M. So, J. -J. Kim, and J. Kim, Phys. Rev. B **66**, 233401 (2002).

[10] H. Mehrez, J. Taylor, H. Guo, J. Wang, and C. Roland, Phys. Rev. Lett. **84**, 2682 (2000).

[11] S. Kokado and K. Harigaya, Phys. Rev. B **69**, 132402 (2004); S. Kokado and K. Harigaya, Synth. Metals **135**, 745 (2003).

[12] For example, see N. Takahashi, H. Ishikuro, and T. Hiramoto, Appl. Phys. Lett. **76**, 209 (2000).

[13] R. V. Giridhar, Jpn. J. Appl. Phys. **35**, 6347 (1996).

[14] S. Kokado and K. Harigaya, J. Phys.: Condens. Matter **15**, 8797 (2003).

[15] The spin polarization is defined by $P_{1(2)} = (D_{1(2),\uparrow} - D_{1(2),\downarrow})/(D_{1(2),\uparrow} + D_{1(2),\downarrow})$, where $D_{1(2),\uparrow}$ is the density-of-states (DOS) at the Fermi level of the FM1(2) for spin-up and $D_{1(2),\downarrow}$ is that of the FM1(2) for spin-down. Also, for the spin polarization at the interfacial layer, the DOS at the interfacial layer is used as $D_{1(2),\uparrow}$. For example, see J. M. De Teresa, A. Barthelemy, A. Fert, J. P. Contour, F. Montaigne, and P. Seneor, Science **286**, 507 (1999).

[16] For carbon nanotubes encapsulating magnetic atoms at the edge, X. X. Zhang, G. H. Wen, S. Huang, L. Dai, R. Gao, Z. L. Wang, J. Magn. Magn. Mater. **231**, L9 (2001).

[17] For carbon nanotubes encapsulating magnetic atoms in the inner region, X. Zhao, S. Inoue, M. Jinno, T. Suzuki, and Y. Ando, Chem. Phys. Lett. **373**, 266 (2003).

[18] T. N. Todorov, G. A. D. Briggs, and A. P. Sutton, J. Phys.: Condens. Matter **5**, 2389 (1993).

[19] S. Kokado, M. Ichimura, T. Onogi, A. Sakuma, R. Arai, J. Hayakawa, K. Ito, and Y. Suzuki, Appl. Phys. Lett. **79**, 3986 (2001).

[20] Y. Ichiyanagi and Y. Kimishima, J. Therm. Anal. Cal., **69**, 919 (2002). As a relevant report, see Y. Ichiyanagi, T. Uozumi, and Y. Kimishima, Trans. Mater. Res. Soc. Jpn. **26** [4], 1097 (2001).

[21] K. Wakabayashi, M. Fujita, H. Ajiki, and M. Sigrist, Phys. Rev. B **59**, 8271 (1999).

[22] J. R. Schrieffer and P. A. Wolff, Phys. Rev. **149**, 491 (1966).

[23] In the previous work [10], t was set to be -2.75 eV.

[24] To approximately describe the s-electron within the tight-binding model, we consider that E_{F} is located near the bottom of an energy dispersion relation. The dispersion relation near the bottom is similar to that of the free electron, which is characteristic of the s-electron. For example, see H. Itoh, A. Shibata, T. Kumazaki, J. Inoue, and S. Maekawa, J. Phys. Soc. Jpn. **68**, 1632 (1999).

[25] Materials with $P_1 \sim 0.45$ correspond nearly to Co, Fe, and $Ni_{80}Fe_{20}$, while $P_2 \sim 0.25$ is Ni. J. S. Moodera and G. Mathon, J. Magn. Magn. Mater. **200**, 248 (1999).

FIGURES

Magnetic atoms

Carbon
nanotube
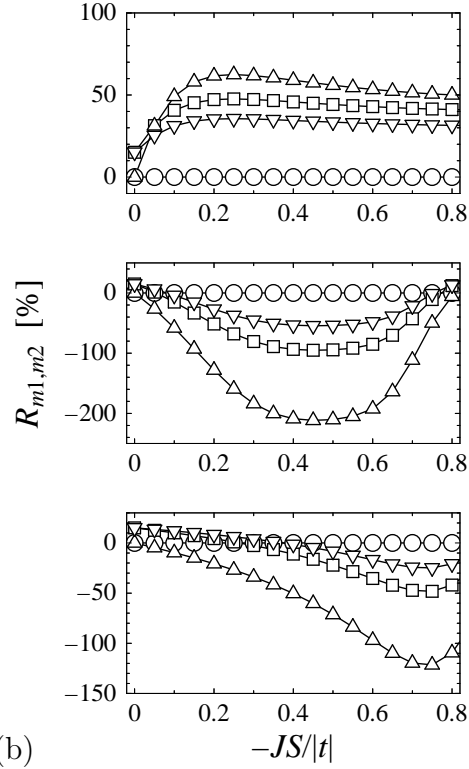
FM1   FM2
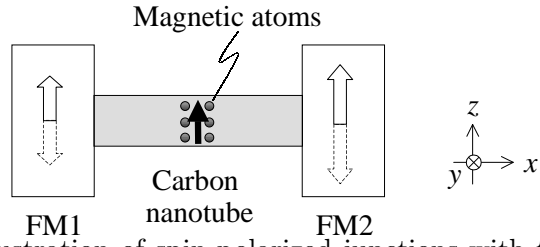
FIG. 1. A schematic illustration of spin-polarized junctions with the carbon nanotube, where magnetic atoms are encapsulated in the center of the nanotube. Electric currents flow in the x-direction.
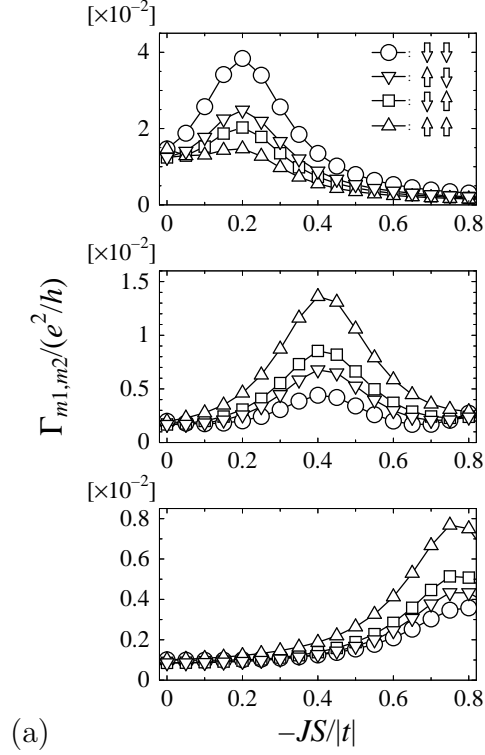
FIG. 2. (a) The conductance $\Gamma_{m1,m2}$ vs $-JS/|t|$ for $\theta=0$ and $\Delta e/|t|=0.2$. The meanings of dots in all panels are $\bigcirc$: $\Gamma_{\Downarrow,\Downarrow}$, $\triangledown$: $\Gamma_{\Uparrow,\Downarrow}$, $\square$: $\Gamma_{\Downarrow,\Uparrow}$, $\triangle$: $\Gamma_{\Uparrow,\Uparrow}$. (b) The MR ratio $R_{m1,m2}$ vs $-JS/|t|$ for $\theta=0$ and $\Delta e/|t|=0.2$. In each figure, the upper, middle, and lower panels are cases of $N=20$, 21, and 22, respectively. The meanings of dots in all panels are $\bigcirc$: $R_{\Downarrow,\Downarrow}$, $\triangledown$: $R_{\Uparrow,\Downarrow}$, $\square$: $R_{\Downarrow,\Uparrow}$, $\triangle$: $R_{\Uparrow,\Uparrow}$.
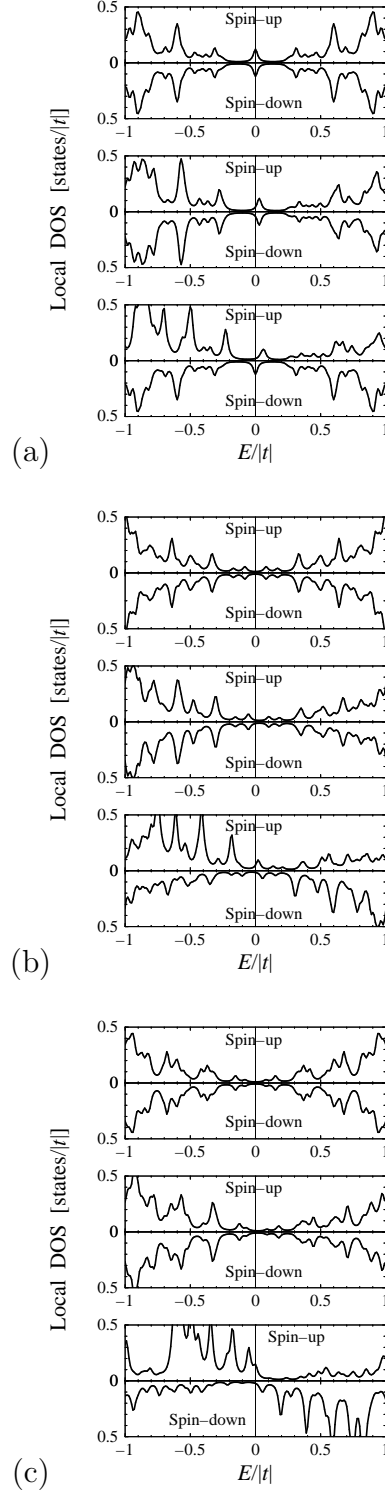
12

FIG. 3. The local DOS in the center of the nanotube, where magnetic atoms are encapsulated. (a) The case of $N=20$. Upper panel: $\Delta e/|t|=0$ and $JS/|t|=0$. Middle panel: $\Delta e/|t|=0.2$ and $JS/|t|=0$. Lower panel: $\Delta e/|t|=0.2$ and $JS/|t|=-0.2$. (b) The case of $N=21$. Upper panel: $\Delta e/|t|=0$ and $JS/|t|=0$. Middle panel: $\Delta e/|t|=0.2$ and $JS/|t|=0$. Lower panel: $\Delta e/|t|=0.2$ and $JS/|t|=-0.4$. (c) The case of $N=22$. Upper panel: $\Delta e/|t|=0$ and $JS/|t|=0$. Middle panel: $\Delta e/|t|=0.2$ and $JS/|t|=0$. Lower panel: $\Delta e/|t|=0.2$ and $JS/|t|=-0.8$. Here, $E_{\mathrm{F}}=0$ is set.
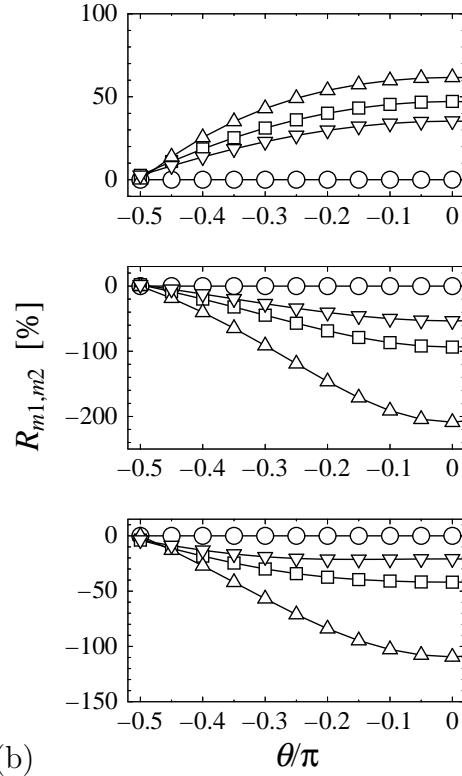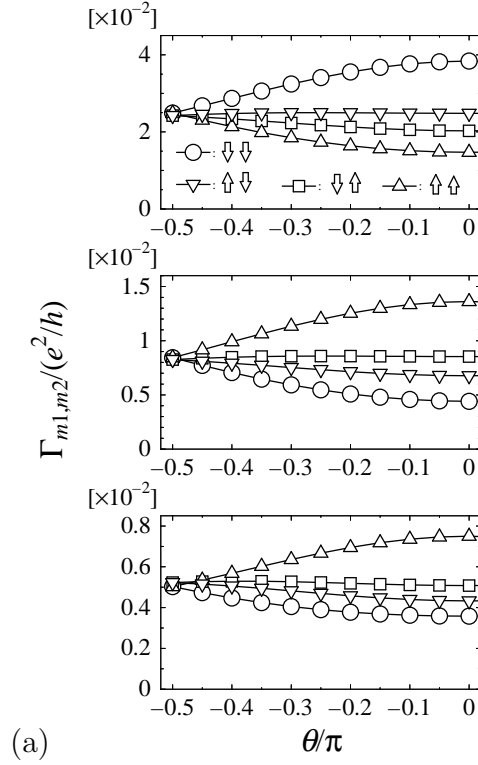
FIG. 4. (a) The conductance $\Gamma_{m1,m2}$ vs θ. The meanings of dots in all panels obey those of Fig. 2(a). (b) The MR ratio $R_{m1,m2}$ vs θ. In each figure, the upper, middle, and lower panels are cases of $JS/|t|=-0.2$ of $N=20$, $JS/|t|=-0.4$ of $N=21$, and $JS/|t|=-0.8$ of $N=22$, respectively. The meanings of dots in all panels obey those of Fig. 2(b).